

HYREC-2: A highly accurate sub-millisecond recombination codeNanoom Lee^{*} and Yacine Ali-Haïmoud[†]*Center for Cosmology and Particle Physics, Department of Physics, New York University,
New York, New York 10003, USA* (Received 3 August 2020; accepted 27 August 2020; published 13 October 2020)

We present the new recombination code HYREC-2, which achieves the same accuracy as the state-of-the-art codes HYREC and COSMOREC and, at the same time, surpasses the computational speed of the code RECFAST commonly used for cosmic microwave background (CMB) anisotropy data analyses. HYREC-2 is based on an effective four-level atom model, accounting exactly for the nonequilibrium of highly excited states of hydrogen, and very accurately for radiative transfer effects with a correction to the Lyman- α escape rate. The latter is computed with the original HYREC and tabulated as a function of temperature, along with its derivatives with respect to the relevant cosmological parameters. This enables the code to keep the same accuracy as the original HYREC over the full 99.7% confidence region of cosmological parameters currently allowed by *Planck*, while running in under one millisecond on a standard laptop. Our code leads to no noticeable bias in any cosmological parameters even in the case of an ideal cosmic-variance-limited experiment up to $\ell = 5000$. Beyond CMB anisotropy calculations, HYREC-2 will be a useful tool to compute various observables that depend on the recombination and thermal history, such as the recombination spectrum or the 21-cm signal.

DOI: [10.1103/PhysRevD.102.083517](https://doi.org/10.1103/PhysRevD.102.083517)**I. INTRODUCTION**

The recombination history of the Universe is a key part of the physics of cosmic microwave background (CMB) anisotropies, the epoch of the dark ages leading to the formation of the first stars, as well as the formation of cosmic structure. When exactly free electrons got bound in the first helium and hydrogen atoms determines the epoch of photon last scattering, and thus the sound horizon. This scale is imprinted into CMB power spectra and the correlation function of galaxies, and serves as a standard ruler [1]. The abundance of free electrons also sets the photon diffusion scale, and hence the damping of small-scale CMB anisotropies [2]. Last, the free-electron fraction determines the epochs of kinematic and kinetic decoupling of baryons from photons, and hence the thermal history of the gas, as well as the formation of the first stars and structures.

The basic physics of hydrogen recombination was laid out in the late 1960s in the seminal works of Peebles [3] and Zeldovich, Kurt, and Sunyaev [4]. Their simple but physically accurate effective three-level model was largely unchanged until the late 1990s (see Ref. [5] for an overview of recombination studies until then), except for improvements in the atomic-physics calculations of case-B recombination coefficients [6]. In 1999, motivated by the

approval of the WMAP [7] and *Planck* [8] satellites, Seager, Sasselov, and Scott conducted the first modern, detailed recombination calculation [9], explicitly accounting for the nonequilibrium of highly excited hydrogen energy levels (but assuming equilibrium among angular momentum substates). They found that the result of their 300-level calculation could be accurately reproduced by an effective three-level atom model, with the case-B recombination coefficient multiplied by a “fudge factor” $F = 1.14$ [10]. This model was implemented in the code RECFAST, which was used for cosmological analyses of WMAP data [11], for which it was sufficiently accurate.

It was realized in the mid 2000s that the RECFAST model for hydrogen recombination would not be sufficiently accurate for the analysis of *Planck* data, as it neglected a variety of physical effects that matter at the required subpercent level of accuracy (see Ref. [12] for an overview of progress by the end of that decade). On the one hand, the angular momentum substates of the excited states of hydrogen are out of equilibrium, which leads to an overall slow down of recombination [13–16]. On the other hand, a variety of radiative transfer effects have to be accounted for, such as feedback from higher-order Lyman transitions, frequency diffusion due to resonant scattering, and two-photon transition from higher levels [17–24].

While conceptually straightforward, the inclusion of hydrogen’s angular momentum substates presented a considerable computational challenge with the standard multilevel method. Indeed, Refs. [15,16] showed that a

^{*}nanoom.lee@nyu.edu
[†]yah2@nyu.edu

recombination history converged at the level needed for *Planck* requires accounting for at least 100 shells of hydrogen energy levels, corresponding to about 5000 separate states. The standard multilevel approach required solving large linear systems at each time step, and even the fastest codes took several hours per recombination history on a standard single-processor machine [16]. This aspect of the recombination problem was solved conclusively a decade ago in Ref. [25], where it was shown that the nonequilibrium dynamics of the excited states can be accounted for *exactly* with an effective few-level atom model (in practice, four levels are enough), with effective recombination coefficients to the lowest excited states accounting for intermediate transitions through the highly excited states (see also Refs. [26,27] for an independent discovery of the method). In contrast with RECFAST’s fudged case-B coefficient, these effective rates are exact, temperature-dependent atomic-physics functions. Once this computational hurdle was cleared, efficient methods to solve the radiative transfer problem were developed shortly thereafter, leading to the fast state-of-the-art public recombination codes HYREC [28] and COSMOREC [29], which achieved excellent agreement with one another despite their different radiative transfer algorithms. The residual theoretical uncertainty of these codes is estimated at the level of a few times 10^{-4} during hydrogen recombination, due to the neglect of subtle radiative transfer effects [30] and collisional transitions [16], whose rates are uncertain.

The accuracy requirement for helium recombination is not as stringent as it is for hydrogen, given that it recombines well before the time at which most CMB photons last scattered. Still, a variety of important radiative transfer effects must be accounted for at the level of accuracy required for *Planck*, such as the photoionization of neutral hydrogen atoms by resonant 584 Å photons and the emission of intercombination-line photons at 591 Å [31–35]. These effects are included numerically in COSMOREC and through fast analytic approximations in HYREC, accurate within 0.3%, which is sufficient for *Planck*. In the rest of this paper, we focus on hydrogen recombination. We defer the task of extending our approach to helium to future work.

Both HYREC and COSMOREC are interfaced with the commonly used Boltzmann codes CAMB [36,37] and CLASS [38], and are able to compute a recombination history in about half a second on a standard laptop. Still, the default code for the cosmological analysis of *Planck* data has remained RECFAST [39], further modified to approximately reproduce the output of HYREC and COSMOREC. The nonequilibrium of angular momentum substates is approximately accounted for by lowering the case-B coefficient fudge factor from 1.14 to 1.125. Radiative transfer physics are approximately mimicked by introducing a double-Gaussian “fudge function,”

correcting the net decay rate in the Lyman- α line.¹ The advantage of this refudged RECFAST over HYREC and COSMOREC remains speed: by not explicitly solving a radiative transfer problem, RECFAST computes a recombination history in about 0.03 seconds on a standard laptop. The recombination calculation is not parallelizable, in contrast with the computation of the transfer functions of independent Fourier modes in a Boltzmann code. Therefore, the additional time spent by HYREC and COSMOREC can be the bottleneck of CMB anisotropy calculations, which may explain the choice of using RECFAST over its more modern, accurate, and versatile counterparts for *Planck* analyses.

As we confirm in this work, the refudged RECFAST is sufficiently accurate for the analysis of *Planck* data, in the sense that it leads to biases in cosmological parameters much smaller than their statistical uncertainties. However, *Planck* is not the final CMB-anisotropy mission: the Simons Observatory [40] and CMB stage-IV [41], which are ground-based surveys, will have more than 10 times better sensitivity with a comparable sky coverage; the proposed CORE satellite [42] will have 10–30 times better sensitivity with full sky coverage. It is unclear whether RECFAST is sufficiently accurate for future CMB missions, nor whether simple additional fudges would be sufficient.

In this paper, we describe the new recombination code HYREC-2², able to compute a recombination history with virtually the same accuracy as the original HYREC, in under 1 millisecond on a standard laptop. Our new code therefore surpasses RECFAST in both accuracy and speed, and ought to become the standard tool for the analysis of future CMB-anisotropy data. HYREC-2 is based on an effective four-level atom model, accounting exactly for the nonequilibrium of excited states of hydrogen [25], and hence accurately capturing the low-redshift tail of recombination, without requiring any fudge factors. Radiative transfer effects are accounted for with a redshift- and cosmology-dependent correction to the Lyman- α net decay rate, exact up to errors quadratic in the deviations of cosmological parameters away from the *Planck* 2018 best-fit cosmology [39]. We check the accuracy of our new code extensively by sampling the full 99.7% confidence region of the *Planck* posterior distribution (assuming a Gaussian distribution), and verifying that the tiny difference with HYREC leads to negligible biases, even for futuristic CMB missions for which RECFAST would be insufficiently accurate.

The rest of this paper is organized as follows. In Sec. II we briefly review hydrogen recombination physics and lay out the exact effective four-level atom equations.

¹To our knowledge, there is no publication describing how the form of the fudge function and the best-fit parameters were determined, nor quantifying the residual error and its impact on cosmological parameter estimation for future experiments.

²HYREC-2 is available at <https://github.com/nanoomlee/HYREC-2>.

In Sec. III we describe HYREC-2, and quantify its accuracy in Sec. IV. We conclude in Sec. V. Appendix A provides explicit equations for the correction functions used in HYREC-2. In Appendix B we provide the equations used in RECFAST in our notation, for completeness and ease of comparison.

II. HYDROGEN RECOMBINATION PHYSICS

A. Recombination phenomenology

The basic phenomenology of hydrogen recombination has been well understood since the late 1960s, with the seminal works of Peebles [3] and Zeldovich, Kurt, and Sunyaev [4]. We briefly summarize the essential physics here (see, e.g., Ref. [43] for more details) and introduce some of the notation along the way.

Direct recombinations to the ground state are ineffective, as the emitted photons almost certainly reionize another hydrogen atom. Therefore, recombinations proceed through the excited states, with principal quantum number $n > 1$. Once an electron and a proton bind together, the newly formed excited hydrogen atom undergoes rapid transitions to other excited states, and eventually either gets photoionized again by thermal CMB photons, or reaches the lowest excited state $n = 2$, with angular momentum sub-states $2s$ and $2p$. The net flow of electrons to the $2s$ and $2p$ states is described by effective recombination coefficients $\mathcal{A}_{2s}(T_m, T_r)$, $\mathcal{A}_{2p}(T_m, T_r)$, which are pure atomic-physics functions depending only on matter and radiation temperatures [25] (see also Refs. [26,27]).

Once in one of the $n = 2$ states, a hydrogen atom has three possible fates. First, it may be directly or indirectly photoionized by thermal CMB photons, with effective photoionization rates $\mathcal{B}_{2s}(T_r)$, $\mathcal{B}_{2p}(T_r)$, depending only on the radiation temperature [25] and related to the effective recombination coefficients through detailed balance relations. Second, it may indirectly transition to the other $n = 2$ state through intermediate transitions to higher excited states; the effective transition rates $\mathcal{R}_{2s,2p}(T_r) = 3\mathcal{R}_{2p,2s}(T_r)$ are also pure functions of atomic physics which only depend on the radiation temperature [25]. Last, but not least, it may decay to the ground state. From the $2p$ state, hydrogen can efficiently decay to the ground state through the allowed Lyman- α transition; this resonant line is highly optically thick, however, and the vast majority of Lyman- α photons end up reexciting another ground-state atom. The net transition rate in the Lyman- α line is, therefore, *approximately* the rate at which photons redshift out of the resonance due to cosmological expansion. For a subpercent accuracy, one must calculate the net decay rate by solving the radiative transfer equation for resonant photons, accounting for feedback from higher-order Lyman lines [17,18], two-photon transitions from higher levels [19,20], time-dependent effects [21], and frequency diffusion in Lyman- α [22–24]. From the $2s$

state, hydrogen may directly decay to the ground state through a “forbidden” two-photon transition. While this transition is optically thin, the net decay rate is affected by the reabsorption of nonthermal photons redshifting out of the Lyman- α resonance [44], and the two-photon transition rate must be computed within the radiative transfer calculation. We denote by $\dot{x}_{2s}|_{1s}$, $\dot{x}_{2p}|_{1s}$ the net rates of change of the fractional populations of $n = 2$ excited states through transitions to the ground state.

At $z \gtrsim 800$, atoms reaching the $n = 2$ states are more likely to be photoionized than reach the ground state. Transitions to the ground state are thus the bottleneck of the recombination process at high redshifts, and as a consequence any error on the rates $\dot{x}_{2s}|_{1s}$, $\dot{x}_{2p}|_{1s}$ directly translates to an error on the overall recombination rate. At $z \lesssim 800$, atoms that reach $n = 2$ almost certainly decay to the ground state before being photoionized, and the recombination dynamics is controlled by the rate of recombinations to excited states, rather than decays to the ground state.

B. General recombination equations

Once helium has fully recombined, the following equation governs the evolution of the free-electron fraction x_e :

$$\dot{x}_e = \sum_{\ell=s,p} (x_{2\ell} \mathcal{B}_{2\ell} - n_{\text{H}} x_e^2 \mathcal{A}_{2\ell}), \quad (1)$$

where n_{H} is the total hydrogen density (both neutral and ionized), and x_{2s} , x_{2p} are the fractional abundances of hydrogen in the first excited states. They are in turn determined by solving the coupled quasi-steady-state rate equations

$$0 \approx \dot{x}_{2\ell} = n_{\text{H}} x_e^2 \mathcal{A}_{2\ell} - x_{2\ell} \mathcal{B}_{2\ell} + x_{2\ell'} \mathcal{R}_{2\ell',2\ell} - x_{2\ell} \mathcal{R}_{2\ell,2\ell'} + \dot{x}_{2\ell}|_{1s}, \quad (2)$$

where $\ell' = p$ if $\ell = s$ and vice versa.

The state-of-the-art recombination codes HYREC [25,28] and COSMOREC [29] accurately compute the rates $\dot{x}_{2\ell}|_{1s}$, and hence the populations of the first excited states $x_{2\ell}$ and the net recombination rate from Eq. (1) in their default modes (in HYREC, the default mode is the “FULL” mode). They do so by solving the time-dependent radiative transfer equation, with different numerical algorithms, and agree with each other within their quoted uncertainty of a few parts in 10^4 . While they are much faster than the previous generation of recombination codes, the ~ 1 second per recombination history can become the bottleneck of CMB power spectra calculations, as it is not parallelizable.

C. Exact effective four-level equations

We may always formally write the net decay rate from 2ℓ to the ground state in the form

$$\dot{x}_{2\ell}|_{1s} = -\mathcal{R}_{2\ell,1s}(z)(x_{2\ell} - g_{2\ell}x_{1s}e^{-E_{21}/T_r}), \quad (3)$$

where $g_{2s} = 1$ and $g_{2p} = 3$ are the statistical weights of the $2s$ and $2p$ states, and $E_{21} \approx 10.2$ eV is the energy difference between the first excited state and the ground state. In contrast with the effective rates $\mathcal{A}_{2\ell}$, $\mathcal{B}_{2\ell}$, and $\mathcal{R}_{2\ell,2\ell'}$, the rates $\mathcal{R}_{2\ell,1s}(z)$ are *not* just functions of temperature: they depend on cosmological parameters through the expansion rate and hydrogen abundance, as well as on the full recombination history up to redshift z , due to the time-dependent nature of radiative transfer.

Inserting Eq. (3) into the steady-state equations, one can find explicit expressions for $x_{2\ell}$:

$$\begin{aligned} x_{2\ell} - g_{2\ell}x_{1s}e^{-E_{21}/T_r} &= \frac{n_{\text{H}}x_e^2\mathcal{A}_{2\ell} - g_{2\ell}x_{1s}e^{-E_{21}/T_r}\mathcal{B}_{2\ell}}{\Gamma_{2\ell} - \mathcal{R}_{2\ell,2\ell'}\mathcal{R}_{2\ell',2\ell}/\Gamma_{2\ell'}} \\ &+ \frac{\mathcal{R}_{2\ell',2\ell}}{\Gamma_{2\ell'}} \times \frac{n_{\text{H}}x_e^2\mathcal{A}_{2\ell'} - g_{2\ell'}x_{1s}e^{-E_{21}/T_r}\mathcal{B}_{2\ell'}}{\Gamma_{2\ell'} - \mathcal{R}_{2\ell',2\ell}\mathcal{R}_{2\ell,2\ell'}/\Gamma_{2\ell'}}, \end{aligned} \quad (4)$$

where $\Gamma_{2\ell}$ is the effective inverse lifetime of 2ℓ ,

$$\Gamma_{2\ell} \equiv \mathcal{B}_{2\ell} + \mathcal{R}_{2\ell,2\ell'} + \mathcal{R}_{2\ell,1s}. \quad (5)$$

Inserting these expressions into Eq. (1), one finds [25]

$$\dot{x}_e = -\sum_{\ell=s,p} C_{2\ell}(n_{\text{H}}x_e^2\mathcal{A}_{2\ell} - g_{2\ell}x_{1s}e^{-E_{21}/T_r}\mathcal{B}_{2\ell}), \quad (6)$$

where the $C_{2\ell}$ factors are given by

$$C_{2\ell} \equiv \frac{\mathcal{R}_{2\ell,1s} + \mathcal{R}_{2\ell,2\ell'}\frac{\mathcal{R}_{2\ell',1s}}{\Gamma_{2\ell'}}}{\Gamma_{2\ell} - \mathcal{R}_{2\ell,2\ell'}\frac{\mathcal{R}_{2\ell',2\ell}}{\Gamma_{2\ell'}}}. \quad (7)$$

The $C_{2\ell}$ factors generalize Peebles' C factor [28]: they represent the effective probabilities that an atom starting in 2ℓ reaches the ground state rather than the continuum, either directly, or after first transitioning to the other $n = 2$ state. This is best seen by rewriting them in the form

$$C_{2\ell} = \frac{\mathcal{R}_{2\ell,1s} + \mathcal{R}_{2\ell,2\ell'}\frac{\mathcal{R}_{2\ell',1s}}{\Gamma_{2\ell'}}}{\mathcal{B}_{2\ell} + \mathcal{R}_{2\ell,2\ell'}\frac{\mathcal{B}_{2\ell'}}{\Gamma_{2\ell'}} + \mathcal{R}_{2\ell,1s} + \mathcal{R}_{2\ell,2\ell'}\frac{\mathcal{R}_{2\ell',1s}}{\Gamma_{2\ell'}}}. \quad (8)$$

These simple equations are *exact*, provided that one uses exact rates $\mathcal{R}_{2\ell,1s}$. They form the basis of HYREC-2, which we describe in the next section.

III. HYREC-2 EQUATIONS

The computational bottleneck of the exact calculation of the recombination history comes from the evaluation of the net decay rates from the first excited states to the ground

state, $\dot{x}_{2s}|_{1s}$ and $\dot{x}_{2p}|_{1s}$, or, equivalently, the coefficients $\mathcal{R}_{2s,1s}$, $\mathcal{R}_{2p,1s}$. The basic idea of HYREC-2 is to use a simple analytic base model for these rates, along with numerical corrections pretabulated with HYREC. We now describe the simple base model.

A. The base approximate model

Neglecting stimulated two-photon decays [19] and the absorption of nonthermal photons redshifted out of the Lyman- α line [44,45], as well as Raman scattering [45] and higher-order Lyman transitions³ [17,18], the net $2s - 1s$ decay rate can be approximated as the spontaneous $2s - 1s$ 2-photon decay rate $\Lambda_{2s,1s}$ [46], as was originally done in Refs. [3,4]:

$$\mathcal{R}_{2s,1s} \approx \Lambda_{2s,1s} \approx 8.22 \text{ s}^{-1}. \quad (9)$$

In the limit of an infinitely narrow Lyman- α resonance, and neglecting corrections due to higher-order two-photon transitions [45,47,48], frequency diffusion [23,24], and feedback from higher-order Lyman transitions [17,18], the net $2p - 1s$ decay rate can be approximately obtained with the Sobolev approximation [9]:

$$\mathcal{R}_{2p,1s} \approx R_{\text{Ly}\alpha} \equiv \frac{8\pi H}{3n_{\text{H}}x_{1s}\lambda_{\text{Ly}\alpha}^3}, \quad (10)$$

where H is the Hubble rate, $\lambda_{\text{Ly}\alpha} \approx 1216 \text{ \AA}$ is the wavelength of the Lyman- α transition, and $x_{1s} \approx 1 - x_e$ is the fraction of hydrogen in the ground state.

HYREC's EMLA2S2P mode consists in solving the four-level equations (6)–(7), with $\mathcal{R}_{2s,1s} = \Lambda_{2s,1s}$ and $\mathcal{R}_{2p,1s} = R_{\text{Ly}\alpha}$. While this mode neglects a variety of radiative transfer effects (listed earlier), it accounts *exactly* for the nonequilibrium of the excited states of hydrogen, up to an arbitrarily high number of states, through the effective rates $\mathcal{A}_{2\ell}$, $\mathcal{B}_{2\ell}$, and $\mathcal{R}_{2\ell,2\ell'}$.

Figure 1 shows the difference between the time derivatives \dot{x}_e in the FULL and EMLA2S2P modes, both evaluated at the same redshift and same value of x_e . We see that the difference becomes negligible at $z \lesssim 800$. This is expected, as at low redshifts the net recombination rate is controlled by the efficiency of recombinations to the excited states (which are modeled exactly through the effective recombination coefficients), rather than decays to the ground state. We see that the *fractional difference* $\Delta\dot{x}_e/\dot{x}_e$ (blue dotted curve) remains at the level of a few percent even at $z \sim 1700$. Nevertheless, the difference $\Delta\dot{x}_e/Hx_e$ (orange solid curve) becomes negligible at $z \gtrsim 1600$. As a consequence, this high-redshift fractional difference does not

³Since the $3p$ state is very nearly in thermal equilibrium with the $2s$ state at early times, Ly- β decays can be recast in terms of effective $2s - 1s$ transitions; see Ref. [28].

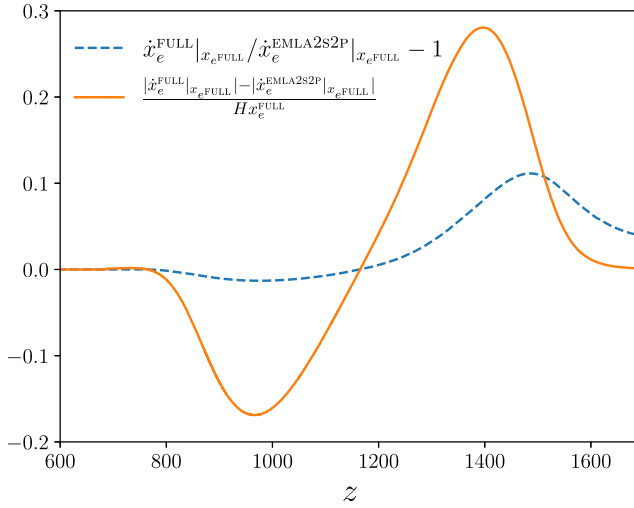


FIG. 1. Blue dotted curve: fractional difference in the rate of change of the free-electron fraction as a function of redshift between HYREC-EMLA2S2P and HYREC-FULL. Note that this difference is computed at the same value of x_e . This difference shows the additional effect of solving radiative transfer equations for the photon population. Orange solid curve: absolute difference in the logarithmic derivative $d \ln x_e / d \ln a = \dot{x}_e / (H x_e)$. This shows that at low redshifts $z \lesssim 800$ and high redshifts $z \gtrsim 1600$ the EMLA2S2P model is accurate enough, but in the intermediate region a detailed radiative transfer calculation is important.

result in significant absolute differences in the free-electron fraction, let alone observable effects in CMB anisotropies.

B. Correction function

The idea behind HYREC-2 is simple: we want to find a correction to the net $2p - 1s$ decay rate that reproduces exact calculations as accurately as possible. Our approach is similar in spirit to the analytic approximations presented in Refs. [23,45], except that the correction we compute is numerical and *exact*, for a given cosmology. Similar corrections are implemented in the current version of RECFAST, as well as in RECFAST++ [29], but our implementation improves on both of these codes in the following ways. First and foremost, the base model of HYREC-2 accounts exactly for the effect of highly excited states, through the effective rates, while the base model of RECFAST and RECFAST++ is Peebles' effective three-level atom. We describe this model in Appendix B for completeness. Second, we *tabulate* the corrections as a function of radiation temperature, rather than fit them with phenomenological functions, as is done in RECFAST. Third, we implement corrections directly at the level of the free-electron fraction *derivative* \dot{x}_e rather than at the level of the free-electron fraction, as done in RECFAST++. Last, but not least, we compute the correction function not just at a fiducial cosmology, but also around it, by also tabulating its derivatives with respect to relevant cosmological parameters.

In more detail, HYREC-2 solves the four-level equations (6)–(7), with

$$\mathcal{R}_{2s,1s} = \Lambda_{2s,1s}, \quad \mathcal{R}_{2p,1s} = \frac{R_{\text{Ly}\alpha}}{1 + \Delta(z)}. \quad (11)$$

The dimensionless correction $\Delta(z)$ is solved for by imposing that $\dot{x}_e^{\text{HYREC-2}}(z, x_e^{\text{FULL}}) = \dot{x}_e^{\text{FULL}}(z, x_e^{\text{FULL}})$. Note that the two derivatives are evaluated at the same value of the free-electron fraction, computed in HYREC's default FULL mode. This enforces that the two solutions are also identical (within machine precision), $x_e^{\text{HYREC-2}} = x_e^{\text{FULL}}$. Given that the EMLA2S2P mode is obtained by setting $\Delta = 0$, the correction Δ is proportional to $\dot{x}_e^{\text{EMLA2S2P}} - \dot{x}_e^{\text{FULL}}$. For completeness, we provide the explicit equation for Δ in Appendix A.

In principle, one could define *two* correction functions: one for the two-photon decay rate $\mathcal{R}_{2s,1s}$ in addition to the correction to the net Lyman- α decay rate $\mathcal{R}_{2p,1s}$. One could solve for the two corrections by imposing that Eq. (4) reproduces the fractional abundances x_{2s} , x_{2p} computed in HYREC's FULL mode. We have opted to not follow this route, however, as one single correction function is sufficient to reproduce the exact \dot{x}_e . Moreover, at $z \gtrsim 800$ the populations of the excited levels depend only weakly on the rates of decay to the ground state, as they are subdominant to photoionizations and indirect transitions to the other excited state, and thus the problem may be numerically ill-posed; in other words, corrections in the $2s - 1s$ and $2p - 1s$ net decay rates are essentially degenerate at high redshift, and thus it is more robust to only compute one single correction.

C. Cosmology dependence

The recombination rate, and thus the correction function $\Delta(z)$, depend not only on redshift, but also on cosmological parameters, through the hydrogen abundance n_{H} , radiation temperature today T_0 , and the Hubble rate H . It was shown in Ref. [49] that the dependence on T_0 can be fully reabsorbed by expressing H and x_e as functions of radiation temperature $T_r = T_0(1+z)$ rather than redshift, and as functions of the baryon-to-photon and matter-to-photon *number ratios*, proportional to the rescaled parameters

$$\hat{\omega}_b \equiv \omega_b (T_0^{\text{FIRAS}} / T_0)^3, \quad (12)$$

$$\hat{\omega}_{cb} \equiv \omega_{cb} (T_0^{\text{FIRAS}} / T_0)^3, \quad (13)$$

where $T_0^{\text{FIRAS}} \equiv 2.7255$ K is the fiducial CMB temperature measured by FIRAS [50], and ω_b , ω_{cb} are the density parameters for baryons and baryons + cold dark matter, respectively.

The Hubble rate, expressed as a function of photon temperature, then only depends on $\hat{\omega}_{cb}$, the effective number of relativistic species N_{eff} (assuming the standard

neutrino-to-photon temperature ratio), and neutrino masses. Given the current upper limits on the sum of neutrino masses $\sum m_\nu < 0.12$ eV [39], neutrinos are relativistic at the relevant redshifts $z \gtrsim 800$, and thus the Hubble rate and Δ is very weakly dependent on $\sum m_\nu$. We checked explicitly that the dependence of Δ on neutrino masses is completely negligible, given the current upper limits.

In principle, the correction function $\Delta(z)$ depends on both $\hat{\omega}_b$ and the helium mass fraction Y_{He} : the hydrogen density is proportional to $\hat{\omega}_H \equiv \hat{\omega}_b(1 - Y_{\text{He}})$, and the evolution of the matter temperature depends on the total number density of free particles, and hence on the helium-to-hydrogen number ratio $f_{\text{He}} = (m_{\text{H}}/m_{\text{He}})Y_{\text{He}}/(1 - Y_{\text{He}})$. However, the matter temperature only starts to depart from the radiation temperature at $z \lesssim 200$, and is in tight equilibrium with it at $z \gtrsim 800$, during which the radiative transfer correction is relevant. The dominant effect of helium abundance variations is therefore included in the parameter $\hat{\omega}_H$, and we do not account for any dependence of $\Delta(z)$ on Y_{He} beyond this parameter. To be clear, the code does self-consistently include the Y_{He} dependence on the matter temperature evolution, but we do not propagate this dependence to $\Delta(z)$, as it is negligible at $z \gtrsim 800$. Throughout this paper, Y_{He} is set by the big bang nucleosynthesis (BBN) constraint [51] and not considered as a free parameter for the bias analysis in Sec. IV C. However, our formulation of the cosmology dependence in terms of $\hat{\omega}_H$ is fully general and allows for arbitrary values of Y_{He} , including outside the BBN relation.

Last, the recombination history can be affected by a variety of processes that might have injected energy, such as particle annihilation [52–54] or decay [55–59], and primordial black hole evaporation [60,61] or accretion [62–64]. These effects are accounted for in HYREC-2 by adding source terms in the differential equations for x_e and T_m (see, e.g., Refs. [54,64] for details). In principle, the correction function Δ also depends on these effects. For instance, Δ does depend on the dark matter annihilation parameter $p_{\text{ann}} = \langle \sigma v \rangle / m_\chi$. We checked explicitly that neglecting this dependence leads to a fractional error in x_e under 3×10^{-4} when p_{ann} is increased up to *Planck*'s 3σ upper limit. This error is comparable to the estimated uncertainty in HYREC and is certainly well below the theoretical uncertainty on the effect of dark matter annihilation on the recombination history. It is therefore safe to neglect the dependence of the correction function on p_{ann} and other energy-injection parameters.

In summary, the correction function $\Delta(z) = \Delta(T_r; \vec{p})$ depends on cosmology through three cosmological parameters, which we group in the vector \vec{p} :

$$\vec{p} \equiv (\hat{\omega}_H, \hat{\omega}_{cb}, N_{\text{eff}}). \quad (14)$$

Since cosmological parameters are already tightly determined by CMB observations, the correction function at any

TABLE I. Cosmological parameters relevant to hydrogen recombination, along with the adopted fiducial values (derived from the *Planck* 2018 results [39]) at which we compute the correction function and its first derivatives. For neutrinos, we adopt the same fiducial cosmological model as the *Planck* Collaboration, with two massless neutrinos, one massive neutrino with mass 0.06 eV, and $N_{\text{eff}} = 3.046$. Note that we only use derivatives of the correction function with respect to $\hat{\omega}_H$, $\hat{\omega}_{cb}$, and N_{eff} , as we found that its dependence on neutrino masses is negligible.

Parameter	Fiducial value
$\hat{\omega}_H \equiv \omega_b(1 - Y_{\text{He}})(T_0^{\text{FIRAS}}/T_0)^3$	0.01689
$\hat{\omega}_{cb} \equiv \omega_{cb}(T_0^{\text{FIRAS}}/T_0)^3$	0.14175
N_{eff}	3.046
$(m_{\nu 1}, m_{\nu 2}, m_{\nu 3})$	(0, 0, 0.06) eV

set of cosmological parameters \vec{p} is well approximated by a linear expansion around the *Planck* best-fit parameters \vec{p}_f , which we refer to as the fiducial model:

$$\Delta(T_r; \vec{p}) \approx \Delta(T_r, \vec{p}_f) + (\vec{p} - \vec{p}_f) \cdot \left. \frac{\partial \Delta}{\partial \vec{p}} \right|_{\vec{p}_f}. \quad (15)$$

We therefore compute and store a total of four functions of radiation temperature or, equivalently, fiducial redshift

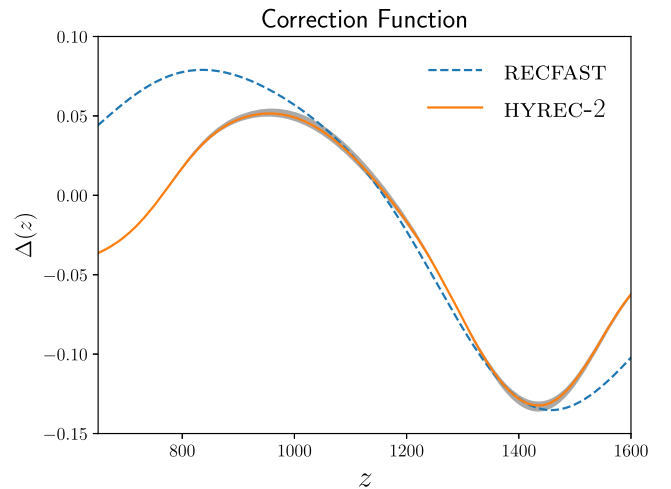


FIG. 2. Correction to the Lyman- α decay rate $\Delta(z)$ for the fiducial cosmology, defined in Eq. (11) (orange). Note that the correction function is technically a function of radiation temperature $\Delta(T_r)$; it is shown as a function of redshift for the fiducial value of $T_0 = T_0^{\text{FIRAS}}$. The gray band shows the span of the correction function when varying cosmological parameters within *Planck*'s full confidence region (see Fig. 4). For reference, the blue dashed curve shows the cosmology-independent fudge function adopted in RECFAST, which is a sum of two Gaussians in redshift. Note that the base models used in HYREC-2 and RECFAST are different, so the two correction functions do not strictly have the same definition; see Appendix B for more details.

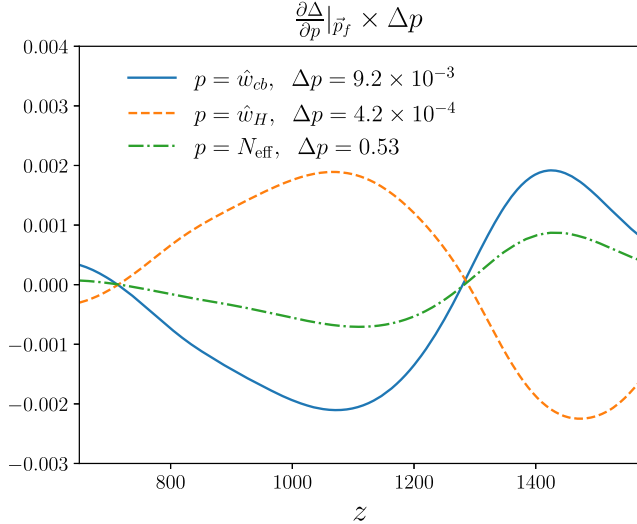


FIG. 3. First derivatives of the correction function $\Delta(z)$ with respect to the three relevant cosmological parameters p , multiplied by Δp corresponding to *Planck*'s 3σ confidence interval.

$z_f \equiv T_r/T_0^{\text{FIRAS}} - 1$. We list the adopted fiducial parameters in Table I. We show the function $\Delta(z, \vec{p})$ for parameters near the fiducial model in Fig. 2, and its derivatives with respect to cosmological parameters in Fig. 3. We tabulate the correction functions over the fiducial redshift range $650 \leq z_f \leq 1620$.

D. Numerical integrator and runtime

The radiative transfer equation solved in HYREC's default FULL mode is a partial differential equation, and as a consequence the time step is tied to the frequency resolution, and must be sufficiently small to ensure convergence. For reference, the default logarithmic step in scale factor is $\Delta \ln a = 8.49 \times 10^{-5}$ (to compute the correction functions at high redshift, we used an even smaller time step for increased accuracy). On the other hand, HYREC-2 only solves an ordinary differential equation (ODE), and the time step can be considerably increased at no noticeable cost in accuracy, provided one uses a sufficiently high-order numerical integrator. We found that we could safely increase the logarithmic step in scale factor to $\Delta \ln a = 4 \times 10^{-3}$ at virtually no loss of accuracy, using a third-order explicit integrator. At early times, when the ODE is stiff, we use an expansion around the Saha equilibrium solution (see Ref. [28]). To make the code stable we use a smaller time step during and slightly after this phase. With our setup, we checked that the fractional difference in x_e due to the increased time step is less than 10^{-4} at all redshifts, comparable to the estimated uncertainty in HYREC.

The simple ODE solved in HYREC-2, combined with a larger time step, considerably reduces the recurring computation time to less than 1 millisecond per

TABLE II. Default run time of each code. Note that this is the *recurring* run time, which does not account for the loading of data in HYREC-2, as this needs to be done once and for all. The run times are calculated on a standard laptop (2.0 GHz Intel i5 processor, 16 GB of RAM).

Code	HYREC	HYREC-2	RECFAST
Run time (ms)	409	0.76	23

cosmological model on a standard laptop; see Table II for a comparison with HYREC-FULL and RECFAST. With this short run time, the recombination history calculation is never the bottleneck of CMB anisotropy Boltzmann codes.

IV. ACCURACY OF HYREC-2

A. Sample cosmologies

To check the accuracy of HYREC-2, we randomly generated 10 000 sample cosmologies from the eight-dimensional Gaussian likelihood derived from the *Planck* 2018 covariance matrix [39] (TT, TE, EE+lowE+lensing+BAO, two-parameter extension),⁴ shown in Fig. 4. As can be seen in Fig. 4, most samples are within the 99.7% confidence region, and there are a handful of samples outside, as expected. We use these sample cosmologies to check the accuracy of HYREC-2 compared to the reference model—the original HYREC.

B. Accuracy of the free-electron fraction

The fractional difference in the free-electron fraction $x_e(z)$ computed in HYREC and HYREC-2 is shown in the top panel of Fig. 5, for a broad range of cosmological parameters. As the plots show, the fractional difference is less than 10^{-4} when cosmological parameters are varied within *Planck*'s 99.7% confidence region. This is lower than the estimated uncertainty in HYREC.

The $\sim 5 \times 10^{-5}$ feature at $z \approx 1600$ is due to the different times at which stiff approximations are turned on, and has no observational consequence whatsoever. Note that even though we neglect the dependence of the correction function on neutrino masses, the code remains accurate even when they are varied away from their fiducial values, within *Planck*'s 3σ limits.

For comparison, we show the fractional difference between RECFAST and HYREC in the lower panel of Fig. 5, for the same parameters. This difference is up to 2 orders of magnitude larger: it gets as large as $\sim 4 \times 10^{-3}$ at $z \gtrsim 200$, and grows to $\sim 1\%$ at $z \lesssim 100$. As we will show in more detail in Sec. IV C, this difference is negligible for

⁴base_nnu_mnu_plikHM_TTTEEE_lowl_lowE_lensing_BAO.covmat from https://wiki.cosmos.esa.int/planck-legacy-archive/index.php/Cosmological_Parameters.

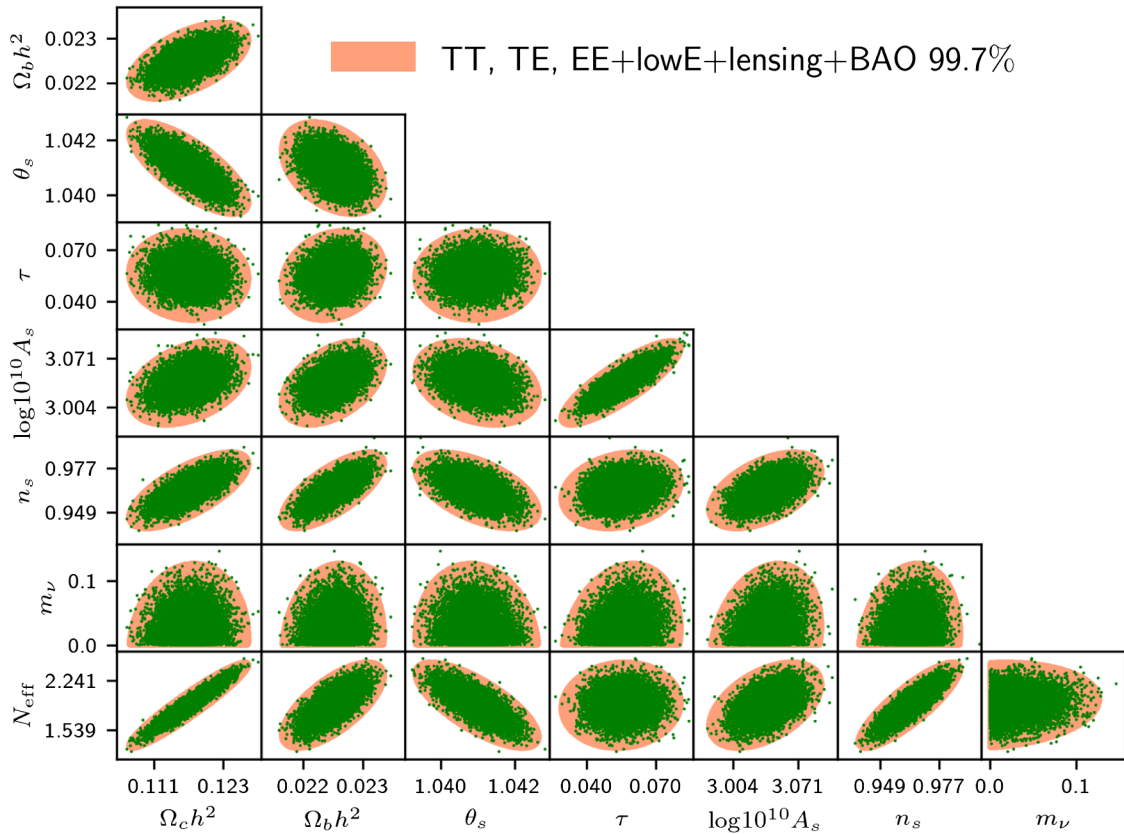


FIG. 4. Ten thousand sample cosmologies used to check the accuracy of HYREC-2, and for the bias analysis in Fig. 7. These samples are drawn from a Gaussian distribution with covariance matrix provided by the *Planck* Collaboration [39]. As expected, most of the samples are within the 99.7% confidence region.

Planck, but can lead to nontrivial biases for next-generation CMB experiments.

C. Bias of cosmological parameters

The metric with which the accuracy of an approximate recombination code is to be measured is the *biases* it induces on cosmological parameters. In the limit of small errors, these biases are directly proportional to the error in CMB anisotropy angular power spectra, C_ℓ . For illustration, we show in Fig. 6 the error in the temperature power spectrum C_ℓ^{TT} for a variety of cosmological parameters varied within the *Planck* 99.7% confidence region. We see that HYREC-2 is more accurate than RECFAST by more than 1 order of magnitude at small angular scales.

We can estimate the biases from a simple Fisher analysis. We denote by $\mathbf{C} \equiv \{C_\ell^{\text{TT}}, C_\ell^{\text{TE}}, C_\ell^{\text{EE}}, C_\ell^{\text{dd}}\}$ the vector containing all the temperature and polarization power spectra and cross-spectra, as well as the power spectrum of lensing deflection. We denote by $\mathbf{\Sigma}$ their covariance matrix, which we describe in more detail below. The chi-square of a set of cosmological parameters \vec{p} is

$$\chi^2(\vec{p}) = (\mathbf{C}(\vec{p}) - \hat{\mathbf{C}}) \cdot \mathbf{\Sigma}^{-1} \cdot (\mathbf{C}(\vec{p}) - \hat{\mathbf{C}}), \quad (16)$$

where $\hat{\mathbf{C}}$ is an estimator of \mathbf{C} constructed from the data, with covariance $\mathbf{\Sigma}$. The best-fit cosmology \vec{p}_{bf} is found by minimizing the χ^2 . Taylor expanding around some fiducial cosmology \vec{p}_0 and neglecting the terms proportional to second derivatives of C_ℓ [65], we get

$$p_{\text{bf}}^i - p_0^i = \mathbf{B}^i(\vec{p}_0) \cdot (\mathbf{C}(\vec{p}_0) - \hat{\mathbf{C}}), \quad (17)$$

$$\mathbf{B}^i \equiv -(F^{-1})^{ij} \frac{\partial \mathbf{C}}{\partial p^j} \cdot \mathbf{\Sigma}^{-1}, \quad (18)$$

where F_{ij} is the Fisher matrix, whose inverse is the covariance of the best-fit cosmological parameters, and whose elements are

$$F_{ij} = \frac{\partial \mathbf{C}}{\partial p^i} \cdot \mathbf{\Sigma}^{-1} \cdot \frac{\partial \mathbf{C}}{\partial p^j}. \quad (19)$$

Suppose the data is a (noisy) realization of the cosmology \vec{p}_0 , i.e., that, upon averaging over realizations, $\langle \hat{\mathbf{C}} \rangle = \mathbf{C}(\vec{p}_0)$. If the theoretical model is unbiased, then the best-fit parameters are also unbiased, i.e., such that, on average over realizations, $\langle \vec{p}_{\text{bf}} - \vec{p}_0 \rangle = 0$.

Now suppose that the theoretical model for $\mathbf{C}(\vec{p})$ has a systematic error $\Delta \mathbf{C}$:

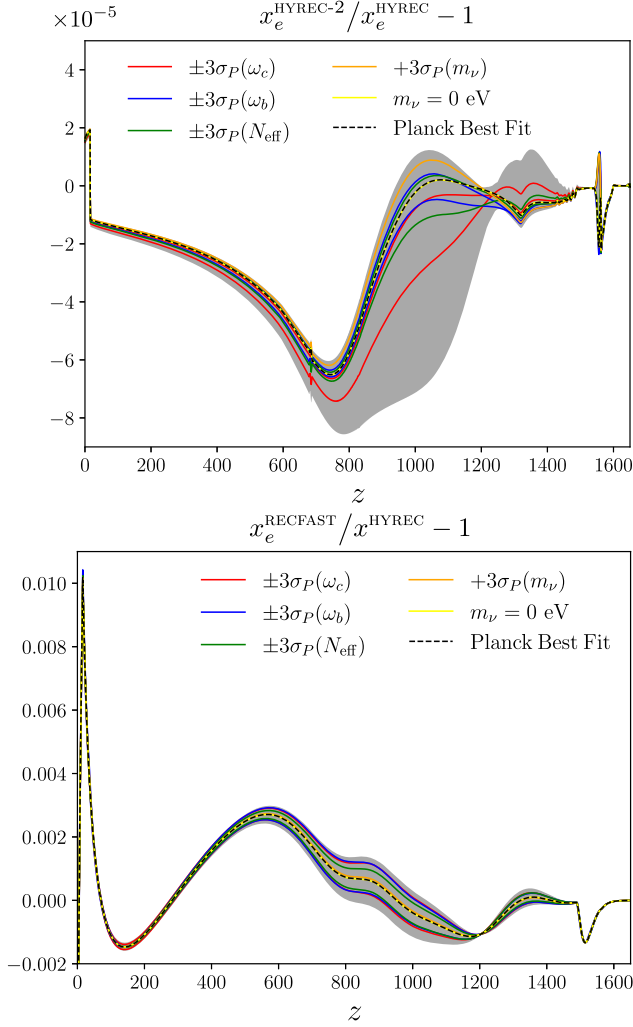


FIG. 5. Fractional differences in the free-electron fraction x_e of HYREC-2 (upper panel) and RECFAST (bottom panel) with respect to the reference model HYREC-FULL. The small ($< 10^{-4}$) fractional difference between HYREC-2 and HYREC for the Planck best-fit cosmology is due to the different time steps in the two codes. (Moreover, the correction function was computed using a higher-accuracy mode of HYREC, with a smaller-than-default time step.) The differences are calculated by changing each parameter with *Planck* $\pm 3\sigma$. The shaded area corresponds to the differences calculated with the 10 000 sample cosmologies shown in Fig. 4.

$$\mathbf{C}(\vec{p}) = \mathbf{C}_{\text{true}}(\vec{p}) + \Delta\mathbf{C}(\vec{p}). \quad (20)$$

The biased theoretical model leads to a *systematic bias* in the best fit, with average

$$\langle p_{\text{bf}}^i - p_0^i \rangle = \mathbf{B}^i(\vec{p}_0) \cdot \Delta\mathbf{C}(\vec{p}_0) \quad (21)$$

$$\approx \mathbf{B}^i(\vec{p}_{\text{fid}}) \cdot \Delta\mathbf{C}(\vec{p}_0), \quad (22)$$

where \mathbf{B}^i was given in Eq. (18). For simplicity, we approximated $\mathbf{B}(\vec{p}_0) \approx \mathbf{B}(\vec{p}_{\text{fid}})$ in Eq. (22); this will not

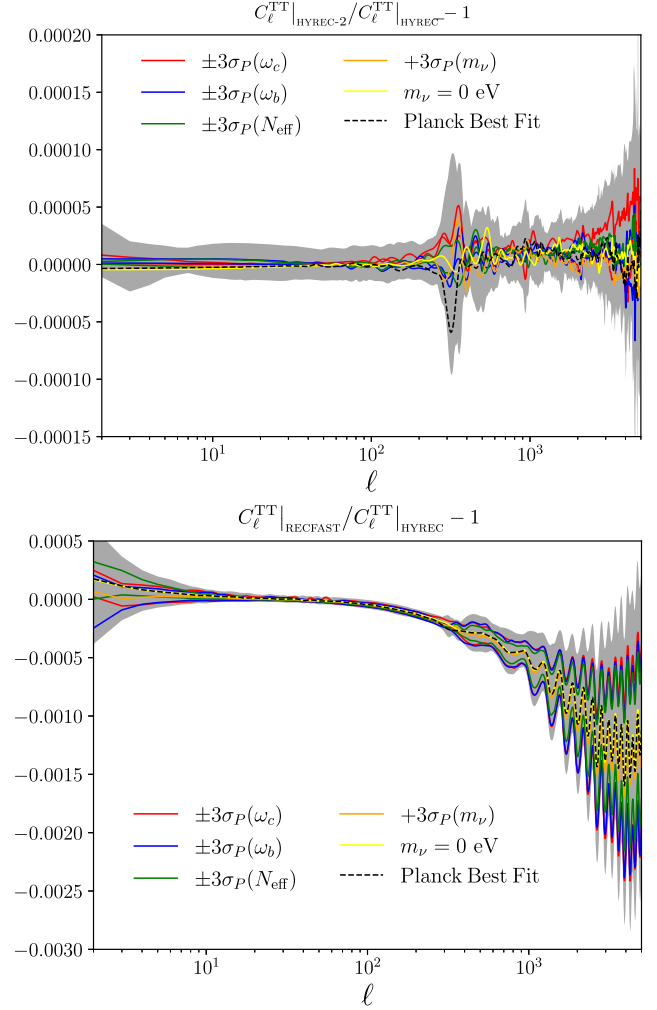


FIG. 6. Fractional error in C_ℓ^{TT} when using HYREC-2 (top) or RECFAST (bottom) instead of HYREC (in its default FULL mode). The shaded area corresponds to the differences calculated with the 10 000 sample cosmologies shown in Fig. 4. In all cases, the C_ℓ 's are computed with the Boltzmann code CLASS [38]. Note that with the default precision settings of CLASS, for a few sample cosmologies the C_ℓ 's show relatively large errors at low ℓ (still $\lesssim 4 \times 10^{-4}$); we checked that these errors disappear once the precision of CLASS is increased.

affect the results since $\Delta\mathbf{C}(\vec{p}_0)$ is already a small quantity. The error to this approximation would be a small correction to a correction. The advantage of this approximation is that we need to compute \mathbf{B} only at the fiducial cosmology.

TABLE III. Noise parameters and the fraction of sky adopted in the Fisher matrix estimates.

Experiment	Stage-IV	CVL
$N_0^{\text{TT}} (\mu\text{K}^2)$	3.38×10^{-7}	0
$N_0^{\text{EE}} (\mu\text{K}^2)$	6.77×10^{-7}	0
θ_T, θ_E (arcmin)	1	$\ell_{\text{max}} = 5000$
f_{sky}	0.4	1

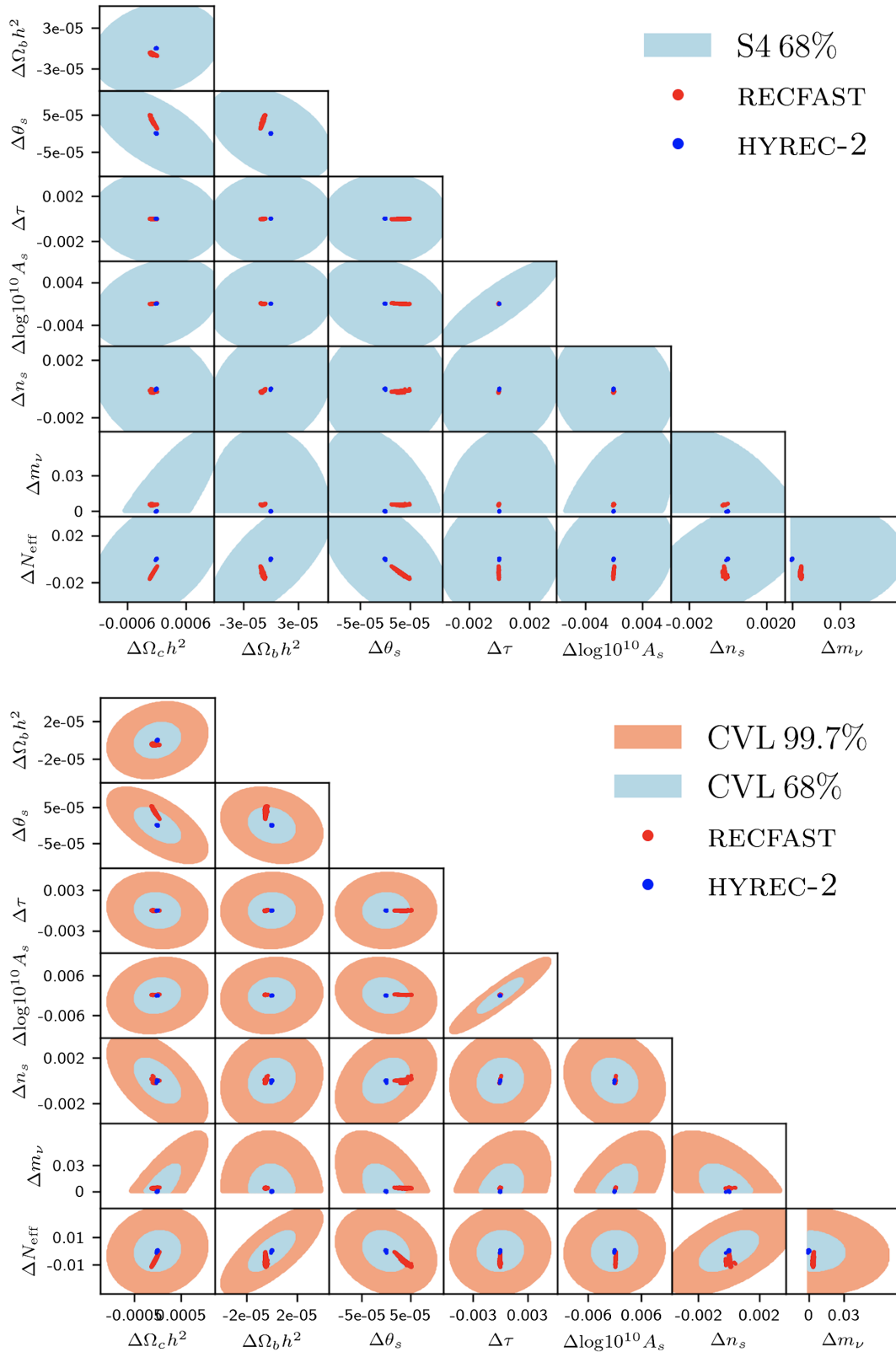


FIG. 7. Bias in cosmological parameters when using HYREC-2 and RECFAST, assuming that HYREC (in its default FULL mode) provides the exact model. The top panel corresponds to CMB Stage-4 settings, and the bottom panel to an idealized CMB experiment, CVL in temperature and polarization up to $\ell_{\text{max}} = 5000$. In both cases, HYREC-2 generates biases that are negligibly small relative to the statistical uncertainty. For a CMB Stage-4 setup, the biases from RECFAST remain within the 68% confidence region. For the CVL experiment, however, RECFAST leads to biases reaching beyond the 68% confidence region in some instances.

Let us now evaluate these systematic biases for a few idealized CMB observations. The covariance matrix Σ has components [66]

$$\begin{aligned} \Sigma_{\ell\ell'}^{XY,WZ} &\equiv \text{cov}[\hat{C}_{\ell}^{XY}, \hat{C}_{\ell'}^{WZ}] \\ &= \delta_{\ell\ell'} \frac{\tilde{C}_{\ell}^{XW}\tilde{C}_{\ell}^{YZ} + \tilde{C}_{\ell}^{XZ}\tilde{C}_{\ell}^{YW}}{f_{\text{sky}}(2l+1)}, \end{aligned} \quad (23)$$

where, for $X = T, E, d$,

$$\tilde{C}_{\ell}^{XW} \equiv C_{\ell}^{XW} + \delta_{XW} N_{\ell}^{XX}, \quad (24)$$

where N_{ℓ}^{XX} is the instrumental noise, of the form [41]

$$N_{\ell}^{XX} = N_0^{XX} \exp\left(\frac{\ell(\ell+1)\theta_x^2}{8 \ln 2}\right). \quad (25)$$

We adopt the noise parameters of Ref. [67] for *Planck* and of Ref. [68] for a CMB Stage-4 (CMB S-4) experiment, which we summarize in Table III. Further, we consider an idealized cosmic-variance-limited (CVL) case for which we assume no instrumental noise in both temperature and polarization up to $\ell = 5000$ and full sky, $f_{\text{sky}} = 1$. In both cases the lensing reconstruction noises are calculated using the code developed in Ref. [69].

We randomly choose various cosmologies from the *Planck* full confidence level (as shown in Fig. 4) and fit each input data (HYREC-FULL mode) to get the best fit of cosmological parameters using each code: RECFAST and HYREC-2. We first checked that if we use the *Planck* settings [39] both codes lead to biases well below statistical uncertainties, which confirms that RECFAST is good enough for *Planck* data as established in Refs. [39,51].

The difference between the best-fit parameters and the input parameters are shown in Fig. 7. The results in the upper panel of Fig. 7 are obtained with the CMB S-4 setting described in Ref. [41], which is $2 \leq \ell \leq 3000$ for *TT* and $2 \leq \ell \leq 5000$ for *TE*, *EE*, and *dd*. The bottom panel shows the corresponding biases for the idealized experiment, assumed to be CVL for $2 \leq \ell \leq 5000$ both in intensity and polarization. Note that in principle the Gaussian approximation for the C_{ℓ} 's (on which the simple χ^2 analysis implicitly relies) is inaccurate at low ℓ ; however, we checked that by changing ℓ_{min} , i.e., $\ell_{\text{min}} = 10$, the low multipoles do not contribute much to the biases and should not greatly affect the answer. We see from Fig. 7 that in some cases biases fall outside of the 68% confidence region of the CVL experiment when using RECFAST. With HYREC-2, all biases remain much smaller than statistical uncertainties for the full range of cosmologies allowed within the 99.7% confidence region of *Planck*.

V. CONCLUSION

We have developed the new recombination code HYREC-2, which combines high accuracy with extreme computational efficiency. This new code is as accurate as the original HYREC across the full range of currently allowed cosmological parameters, and is 30 times faster than RECFAST, with a recurring runtime under one millisecond on a standard laptop. This makes HYREC-2 the fastest recombination code currently available, by far.

HYREC-2 is based on an effective four-level atom model, which exactly captures the late-time ($z \lesssim 800$) recombination dynamics. Radiative transfer effects, which are relevant at early times, are accounted for through a numerical correction to the Lyman- α net decay rate, tabulated as a function of temperature using HYREC. In order to achieve sub-0.01% accuracy across a broad range of cosmologies, we also tabulated the derivatives of the correction function with respect to cosmological parameters. We have checked explicitly that the $\sim 10^{-4}$ fractional differences with HYREC result in no bias for any cosmological parameters for current, planned, and even futuristic CMB missions, for which RECFAST would not be sufficiently accurate.

Our new recombination code will be most useful for fast and accurate CMB-anisotropy calculations, which are required to extract unbiased cosmological parameters from CMB anisotropy data. In addition, it will be a key tool to study the CMB signatures of dark matter decay or annihilation [52–54], other sources of energy injection [55,59,64], or in general any nonstandard physics that may affect the recombination and thermal history [70].

Last, but not least, in combination with the effective conductance method [71] HYREC-2 can be used to efficiently compute the cosmological recombination spectrum [72]. This minute but rich signal is a guaranteed distortion to the CMB blackbody spectrum [13,73]. Looking ahead, it may eventually become a powerful probe of the early Universe [74–77], complementing CMB anisotropies and opening up a new window into the Universe's early thermal history.

ACKNOWLEDGMENTS

We thank Jens Chluba, Antony Lewis, and Julien Lesgourgues for useful conversations. This work is supported by NSF Grant No. 1820861 and NASA Grant No. 80NSSC20K0532.

APPENDIX A: EXPLICIT EXPRESSION FOR THE CORRECTION FUNCTION

Equation (6) can be rewritten as $\dot{x}_{\ell} = -\sum_{\ell'} C_{2\ell} X_{2\ell'}$, where

$$X_{2\ell} \equiv n_{\text{H}} x_e^2 \mathcal{A}_{2\ell} - g_{2\ell} x_{1s} e^{-E_{21}/T_r} \mathcal{B}_{2\ell}. \quad (\text{A1})$$

In HYREC-2, $\mathcal{R}_{2s,1s} = \Lambda_{2s,1s}$ and $\mathcal{R}_{2p,1s} = R_{Ly\alpha}/(1 + \Delta)$; the EMLA2S2P mode has $\Delta = 0$. We therefore have

$$\dot{x}_e^{\text{HYREC-2}}(\Delta) = \frac{\dot{x}_e^{\text{EMLA}} + A\Delta}{1 + B\Delta}, \quad (\text{A2})$$

with

$$A = -\frac{\Lambda_{2s,1s}[(\mathcal{B}_{2p} + \mathcal{R}_{2p,2s})X_{2s} + \mathcal{R}_{2p,2s}X_{2p}]}{\Gamma_{2s}\Gamma_{2p} - \mathcal{R}_{2s,2p}\mathcal{R}_{2p,2s}}, \quad (\text{A3})$$

$$B = \frac{\Gamma_{2s}(\mathcal{B}_{2p} + \mathcal{R}_{2p,2s}) - \mathcal{R}_{2s,2p}\mathcal{R}_{2p,2s}}{\Gamma_{2s}\Gamma_{2p} - \mathcal{R}_{2s,2p}\mathcal{R}_{2p,2s}}. \quad (\text{A4})$$

The correction Δ is set such that $\dot{x}_e^{\text{HYREC-2}}(\Delta) = \dot{x}_e^{\text{FULL}}$. Solving, we find

$$\Delta = \frac{\dot{x}_e^{\text{EMLA}} - \dot{x}_e^{\text{FULL}}}{B\dot{x}_e^{\text{FULL}} - A}. \quad (\text{A5})$$

APPENDIX B: EQUATIONS FOR RECFAST IN OUR NOTATION

1. Peebles' effective three-level model

Peebles' effective three-level model [3] relies on two additional assumptions relative to the effective four-level model that we use. First, the two states $2s$, $2p$ are assumed to be in thermal equilibrium, $x_{2s} = x_{2p}/3 \equiv x_2/4$, with $x_2 \equiv x_{2s} + x_{2p}$. The recombination rate (1) then simplifies to

$$\dot{x}_e = x_2\mathcal{B}_B - n_H x_e^2 \mathcal{A}_B, \quad (\text{B1})$$

$$\mathcal{B}_B \equiv \frac{1}{4}(\mathcal{B}_{2s} + 3\mathcal{B}_{2p}), \quad (\text{B2})$$

$$\mathcal{A}_B \equiv \mathcal{A}_{2s} + \mathcal{A}_{2p}. \quad (\text{B3})$$

The population x_2 of the first excited state is then obtained by solving the steady-state equation,

$$\begin{aligned} 0 \approx \dot{x}_2 &= n_H x_e^2 \mathcal{A}_B - x_2 \mathcal{B}_B + \dot{x}_{2s}|_{1s} + \dot{x}_{2p}|_{1s} \\ &\approx n_H x_e^2 \mathcal{A}_B - x_2 \mathcal{B}_B + \frac{1}{4}(\Lambda_{2s,1s} + 3R_{Ly\alpha}) \\ &\quad \times (4x_{1s}e^{-E_{21}/T_r} - x_2), \end{aligned} \quad (\text{B4})$$

where here again we used the simple approximations (9) and (10) for the net decay rates to the ground state. This equation can be easily solved for x_2 , which, upon insertion into Eq. (B1), gives the closed form

$$\dot{x}_e = -C(n_H x_e^2 \mathcal{A}_B - 4x_{1s}\mathcal{B}_B e^{-E_{21}/T_r}), \quad (\text{B5})$$

where the Peebles C factor is given by

$$C \equiv \frac{\Lambda_{2s,1s} + 3R_{Ly\alpha}}{4\mathcal{B}_B + \Lambda_{2s,1s} + 3R_{Ly\alpha}}. \quad (\text{B6})$$

This result can also be obtained from Eqs. (6) and (8) using the detailed balance relation $\mathcal{R}_{2s,2p} = 3\mathcal{R}_{2p,2s}$, and assuming that $\mathcal{R}_{2s,2p} \gg \Lambda_{2s,1s} + \mathcal{B}_{2s}$ and $\mathcal{R}_{2p,2s} \gg R_{Ly\alpha} + \mathcal{B}_{2p}$. This assumption is required to enforce equilibrium between $2s$ and $2p$ regardless of the relative values of the other rates, and implies $C_{2s} = C_{2p} = C$. In practice, it does not hold at low enough temperature, $z \lesssim 700$.

In addition to this equilibrium assumption, the effective rates $\mathcal{A}_B(T_m, T_r)$ and $\mathcal{B}(T_r)$ are approximated as follows:

$$\mathcal{A}_B(T_m, T_r) \approx \alpha_B(T_m) \equiv \mathcal{A}_B(T_m, 0), \quad (\text{B7})$$

$$\mathcal{B}_B(T_r) \approx \beta_B(T_r) \equiv \frac{(2\pi\mu_e T_r)^{3/2}}{4h^3} e^{E_2/T_r} \alpha_B(T_r), \quad (\text{B8})$$

where $E_2 \approx -3.4$ eV is the energy of the first excited state. In other words, the effective recombination coefficient is computed in the zero-radiation-temperature limit and the photoionization rate is assumed to be given by detailed balance, even though this is not self-consistent with the zero-radiation-temperature assumption.

2. Fudge factors and functions

Since the zero-radiation-temperature effective recombination coefficient systematically underestimates the exact effective recombination coefficient, the code RECFAST introduces a ‘‘fudge factor’’ $F > 1$, and substitutes $\alpha_B \rightarrow F \times \alpha_B$. The fudge factor was first estimated as $F \approx 1.14$ when enforcing equilibrium between angular momentum substates of excited states [9,10]. Based on the study of Ref. [12], which accounts for the nonequilibrium of angular momentum substates, the current version of RECFAST uses an updated fudge factor $F \approx 1.125$. It was shown in Ref. [25] that \mathcal{A}_B/α_B indeed lies in the range 1.12–1.14, though it is not a constant, but rather depends on redshift.

The latest version of RECFAST corrects the net decay rate in Lyman- α which is in our Eq. (11). (Note, however, that the base model is different.) The function $\Delta(z)$ is a sum of two Gaussians, whose amplitudes and widths were chosen to best mimic detailed calculations of HYREC and COSMOREC.

It should be clear that the three-level simplification (and especially the fudging of \mathcal{A}_B) *does not provide any computational advantage* over the already very simple effective four-level model on which HYREC-2 is based.

- [1] D. J. Eisenstein, W. Hu, and M. Tegmark, *Astrophys. J. Lett.* **504**, L57 (1998).
- [2] J. Silk, *Astrophys. J.* **151**, 459 (1968).
- [3] P. J. E. Peebles, *Astrophys. J.* **153**, 1 (1968).
- [4] Y. B. Zel'dovich, V. G. Kurt, and R. A. Sunyaev, *J. Exp. Theor. Phys.* **28**, 146 (1969), <https://ui.adsabs.harvard.edu/abs/1969JETP...28..146Z/abstract>.
- [5] W. Hu, D. Scott, N. Sugiyama, and M. White, *Phys. Rev. D* **52**, 5498 (1995).
- [6] D. Pequignot, P. Petitjean, and C. Boisson, *Astron. Astrophys.* **251**, 680 (1991), <http://adsabs.harvard.edu/full/1991A%26A...251..680P>.
- [7] C. L. Bennett *et al.*, *Astrophys. J.* **583**, 1 (2003).
- [8] Planck Collaboration, [arXiv:astro-ph/0604069](https://arxiv.org/abs/astro-ph/0604069).
- [9] S. Seager, D. D. Sasselov, and D. Scott, *Astrophys. J. Suppl. Ser.* **128**, 407 (2000).
- [10] S. Seager, D. D. Sasselov, and D. Scott, *Astrophys. J.* **523**, L1 (1999).
- [11] G. Hinshaw *et al.*, *Astrophys. J. Suppl. Ser.* **208**, 19 (2013).
- [12] J. A. Rubiño-Martín, J. Chluba, W. A. Fendt, and B. D. Wandelt, *Mon. Not. R. Astron. Soc.* **403**, 439 (2010).
- [13] J. A. Rubiño-Martín, J. Chluba, and R. A. Sunyaev, *Mon. Not. R. Astron. Soc.* **371**, 1939 (2006).
- [14] J. Chluba, J. A. Rubiño-Martín, and R. A. Sunyaev, *Mon. Not. R. Astron. Soc.* **374**, 1310 (2007).
- [15] D. Grin and C. M. Hirata, *Phys. Rev. D* **81**, 083005 (2010).
- [16] J. Chluba, G. M. Vasil, and L. J. Dursi, *Mon. Not. R. Astron. Soc.* **407**, 599 (2010).
- [17] J. Chluba and R. A. Sunyaev, *Astron. Astrophys.* **475**, 109 (2007).
- [18] E. E. Kholupenko, A. V. Ivanchik, and D. A. Varshalovich, *Phys. Rev. D* **81**, 083004 (2010).
- [19] J. Chluba and R. A. Sunyaev, *Astron. Astrophys.* **446**, 39 (2006).
- [20] V. K. Dubrovich and S. I. Grachev, [arXiv:astro-ph/0501672](https://arxiv.org/abs/astro-ph/0501672).
- [21] J. Chluba and R. A. Sunyaev, *Astron. Astrophys.* **496**, 619 (2009).
- [22] S. I. Grachev and V. K. Dubrovich, *Astron. Lett.* **34**, 439 (2008).
- [23] C. M. Hirata and J. Forbes, *Phys. Rev. D* **80**, 023001 (2009).
- [24] J. Chluba and R. A. Sunyaev, *Astron. Astrophys.* **503**, 345 (2009).
- [25] Y. Ali-Haïmoud and C. M. Hirata, *Phys. Rev. D* **82**, 063521 (2010).
- [26] M. S. Burgin, *Bull. Lebedev Phys. Inst.* **36**, 110 (2009).
- [27] M. S. Burgin, *Bull. Lebedev Phys. Inst.* **37**, 280 (2010).
- [28] Y. Ali-Haïmoud and C. M. Hirata, *Phys. Rev. D* **83**, 043513 (2011).
- [29] J. Chluba and R. M. Thomas, *Mon. Not. R. Astron. Soc.* **412**, 748 (2011).
- [30] Y. Ali-Haïmoud, D. Grin, and C. M. Hirata, *Phys. Rev. D* **82**, 123502 (2010).
- [31] E. R. Switzer and C. M. Hirata, *Phys. Rev. D* **77**, 083006 (2008).
- [32] C. M. Hirata and E. R. Switzer, *Phys. Rev. D* **77**, 083007 (2008).
- [33] E. R. Switzer and C. M. Hirata, *Phys. Rev. D* **77**, 083008 (2008).
- [34] J. A. Rubiño-Martín, J. Chluba, and R. A. Sunyaev, *Astron. Astrophys.* **485**, 377 (2008).
- [35] E. E. Kholupenko, A. V. Ivanchik, and D. A. Varshalovich, *Astron. Lett.* **34**, 725 (2008).
- [36] A. Lewis, A. Challinor, and A. Lasenby, *Astrophys. J.* **538**, 473 (2000).
- [37] C. Howlett, A. Lewis, A. Hall, and A. Challinor, *J. Cosmol. Astropart. Phys.* **04** (2012) 027.
- [38] J. Lesgourgues, [arXiv:1104.2932](https://arxiv.org/abs/1104.2932).
- [39] N. Aghanim *et al.* (Planck Collaboration), [arXiv:1807.06209](https://arxiv.org/abs/1807.06209).
- [40] Simons Observatory Collaboration, *J. Cosmol. Astropart. Phys.* **02** (2019) 056.
- [41] K. N. Abazajian *et al.* (CMB-S4 Collaboration), [arXiv:1610.02743](https://arxiv.org/abs/1610.02743).
- [42] C. Armitage-Caplan, M. Avillez, D. Barbosa, A. Banday, N. Bartolo *et al.* (Core Collaboration), [arXiv:1102.2181](https://arxiv.org/abs/1102.2181).
- [43] Y. Ali-Haïmoud, Ph.D. thesis, California Institute of Technology, 2011.
- [44] E. E. Kholupenko and A. V. Ivanchik, *Astron. Lett.* **32**, 795 (2006).
- [45] C. M. Hirata, *Phys. Rev. D* **78**, 023001 (2008).
- [46] S. P. Goldman, *Phys. Rev. A* **40**, 1185 (1989).
- [47] J. Chluba and R. A. Sunyaev, *Astron. Astrophys.* **512**, A53 (2010).
- [48] J. Chluba and R. A. Sunyaev, *Astron. Astrophys.* **480**, 629 (2008).
- [49] M. M. Ivanov, Y. Ali-Haïmoud, and J. Lesgourgues, [arXiv:2005.10656](https://arxiv.org/abs/2005.10656) [*Phys. Rev. D* (to be published)].
- [50] D. J. Fixsen, *Astrophys. J.* **707**, 916 (2009).
- [51] P. A. R. Ade *et al.* (Planck Collaboration), *Astron. Astrophys.* **594**, A13 (2016).
- [52] J. Chluba, *Mon. Not. R. Astron. Soc.* **402**, 1195 (2010).
- [53] N. Padmanabhan and D. P. Finkbeiner, *Phys. Rev. D* **72**, 023508 (2005).
- [54] G. Giesen, J. Lesgourgues, B. Audren, and Y. Ali-Haïmoud, *J. Cosmol. Astropart. Phys.* **12** (2012) 008.
- [55] J. A. Adams, S. Sarkar, and D. W. Sciama, *Mon. Not. R. Astron. Soc.* **301**, 210 (1998).
- [56] L. Zhang, X. Chen, M. Kamionkowski, Z. G. Si, and Z. Zheng, *Phys. Rev. D* **76**, 061301 (2007).
- [57] M. Mapelli, A. Ferrara, and E. Pierpaoli, *Mon. Not. R. Astron. Soc.* **369**, 1719 (2006).
- [58] E. Pierpaoli, *Phys. Rev. Lett.* **92**, 031301 (2004).
- [59] X.-L. Chen and M. Kamionkowski, *Phys. Rev. D* **70**, 043502 (2004).
- [60] V. Poulin, J. Lesgourgues, and P. D. Serpico, *J. Cosmol. Astropart. Phys.* **03** (2017) 043.
- [61] H. Poulter, Y. Ali-Haïmoud, J. Hamann, M. White, and A. G. Williams, [arXiv:1907.06485](https://arxiv.org/abs/1907.06485).
- [62] M. C. Miller, *Astrophys. J.* **544**, 43 (2000).
- [63] M. Ricotti, J. P. Ostriker, and K. J. Mack, *Astrophys. J.* **680**, 829 (2008).
- [64] Y. Ali-Haïmoud and M. Kamionkowski, *Phys. Rev. D* **95**, 043534 (2017).
- [65] S. Dodelson, *Modern Cosmology* (Academic Press, Amsterdam, 2003).
- [66] A. Benoit-Levy, K. M. Smith, and W. Hu, *Phys. Rev. D* **86**, 123008 (2012).
- [67] J. R. Shaw and J. Chluba, *Mon. Not. R. Astron. Soc.* **415**, 1343 (2011).

- [68] D. Green, J. Meyers, and A. van Engelen, *J. Cosmol. Astropart. Phys.* **12** (2017) 005.
- [69] J. Peloton, M. Schmittfull, A. Lewis, J. Carron, and O. Zahn, *Phys. Rev. D* **95**, 043508 (2017).
- [70] Y. Ali-Haïmoud, C. M. Hirata, and M. Kamionkowski, *Phys. Rev. D* **83**, 083508 (2011).
- [71] Y. Ali-Haïmoud, *Phys. Rev. D* **87**, 023526 (2013).
- [72] J. Chluba and Y. Ali-Haïmoud, *Mon. Not. R. Astron. Soc.* **456**, 3494 (2016).
- [73] R. A. Sunyaev and J. Chluba, in *Frontiers of Astrophysics: A Celebration of NRAO's 50th Anniversary*, edited by A. H. Bridle, J. J. Condon and G. C. Hunt, ASPCS, Vol. 395 (Astronomical Society of the Pacific, San Francisco, 2008) p. 35.
- [74] J. Chluba, M. H. Abitbol, N. Aghanim, Y. Ali-Haimoud, M. Alvarez *et al.*, [arXiv:1909.01593](https://arxiv.org/abs/1909.01593).
- [75] J. Chluba, A. Kogut, S. P. Patil, M. H. Abitbol, N. Aghanim, and Y. Ali-Haimoud *et al.*, *Astro 2020 White Paper* **51**, 184 (2019), <https://arxiv.org/abs/1903.04218>.
- [76] J. Delabrouille, M. H. Abitbol, N. Aghanim, Y. Ali-Haimoud, D. Alonso *et al.*, [arXiv:1909.01591](https://arxiv.org/abs/1909.01591).
- [77] D. Sarkar and R. Khatri, *J. Cosmol. Astropart. Phys.* **01** (2020) 050.